

NEURAL NETWORK MODELING OF RELATIVE HUMIDITY AND TEMPERATURE DISTRIBUTION OVER NIGERIA

¹Ibeh G. F., ²Ibeh L. M., ³Ogbonna R. C., ⁴Ofoma J. N and ⁵Akande S

¹Department of Physics with Electronics, Evangel University Akaeze Ebonyi State, Nigeria;

²Department of Geography and Environmental Sciences, Ludwig-Maximilians, University of Munich, Germany

^{3,4}Department of Computer Science and Mathematics, Evangel University Akaeze, Ebonyi State, Nigeria;

⁵Centre for Space Research and Application, Federal University of Technology Akure, Nigeria

Abstract

This paper used neural network model to study the distributions of relative humidity and temperature over Nigeria. The theoretical explorations of the relationship between the parameters were reviewed. This study was carried out on thirty-six point stations over Nigeria. Temporal variations of estimation and prediction of relative humidity and temperature were carried out in this study. The results revealed that temperature and relative humidity distributions over Nigeria are in variant. They were inversely proportional to each other as affirmed by other researched. Spatio-temporal variations revealed that relative humidity is higher in wet seasons compared to dry seasons in Nigeria. It is also higher within the Southern part of Nigeria as a result of coastal nature, moisture content in the atmosphere of the region and low temperature gradient. The influences of temperature on relative humidity were study. The results shows inversion with the rates of relative humidity and the rates of temperature both in wet and dry seasons, and within the Southern and Northern part of Nigeria. This could be because increase in temperature raises saturated vapour pressure, which leads to reduction in the relative humidity. The variation of temperature may be due to diabatic heating and adiabatic effects in the atmosphere. Based on the similar signatures of the estimated and observed temporal distributions of the parameters, forecast of two years ahead of the years of the study were successfully achieved. The result showed strong negative relationship between temperature and relative humidity. The correlation coefficient is calculated to be -0.94. This strong negative correlation signifies that as the temperature decreases, the relative humidity increase (and vice versa). The performance of neural network model in the distributions shows the ability of the model in studying atmospheric parameters as confirmed by other researchers.

Keywords: Relative Humidity, Temperature, Neural Network, Diabatic, Adiabatic and Nigeria

1. Introduction

Urban migration has contributed to the urban-rural contrast regarding atmospheric humidity across the globe [1]. According to [2] relative humidity can define as the ratio of the actual water vapour pressure (e) to the equilibrium vapour pressure over a saturation vapor pressure (e_s). That is the ratio of the actual water vapour dry mass mixing ratio (w) to the saturation mixing ratio (w_s) at the ambient temperature and pressure. That is the ratio between the actual vapour content of the air and the vapour content of air at the same temperature saturated with water vapour. If the temperature of air rises and no change occurs in its vapour content, then the relative humidity is lowered, while the absolute humidity remains the same. A fall in temperature increases the relative humidity vice versa [3]. Relative humidity is increased due to evaporation, sublimation

Corresponding Author: Ibeh G.F., Email: ibehgabrielfriday@evangeluniversity.edu.ng, Tel: +2348065289990

Journal of the Nigerian Association of Mathematical Physics Volume 63, (Jan. – March, 2022 Issue), 147 –158

and melting process. In this process, heat is removed from the environments, which result to decrease in temperature and increases in relative humidity. Again, water vapour is released during evaporation and sublimation, this result to increase in specific humidity [4]. The concentrations of relative humidity are always high in wet season due to high moisture content in the atmosphere. It is also higher in the coastal region (South) of Nigeria both in wet and dry season because of the moistness and humidity in the region [3]. The nonlinear nature of relative humidity makes it a challenging task for prediction. In recent researches, machine learning-based prediction strategies have proven significant attention in tackling the challenges of nonlinear and complex problems of relative humidity [5, 6].

Machine learning is the process of pattern recognition and computational learning theory in artificial intelligence. It is the learning and buildings of algorithms that can learn from or detect patterns and make predictions on the data sets [7, 8, 9]. Machine learning involves two types of tasks, supervised and unsupervised. Supervised machine learning pre-defined set of training examples, which then facilitate its ability to reach an accurate conclusion when given new data, while in unsupervised machine learning, the program is given a bunch of data and must find patterns and relationships therein [8, 9].

Artificial neural network (ANN) also known as neural network (NN) is one of the major types of machine learning. Machine learning-based models have been widely used for environmental and atmospheric data modeling, estimation and prediction [10, 11, 12, 13]. An NN is an interconnected network of processing units emulating the network of neurons in the brain [8, 9]. Neural Networks (NN) are important data mining tool which build networks that will mimic brain activities and be able to learn. NN usually learns by examples, if NN is supplied with enough examples, it should be able to perform classification and even discover new trends or patterns in the data. Basic NN is composed of three layers, input, output and hidden layer. Each layer can have number of nodes that can be connected from input to output layers through the hidden layers [14]. There are no specific or perfect rules for deciding the most appropriate number of neurons in a hidden layer [15]. [16] and [4] reveal that NN is an impressive tool in modeling climatic parameters such as temperature, relative humidity and solar radiation. We are using neural network to study the relationship between relative humidity with temperature. We also study the spatio-temporal distributions of the parameters over Nigeria.

1.1 Theoretical Background of the relation between Relative humidity, Temperature and Specific Humidity at lower Atmosphere

The expressions below show the theoretical relation between atmospheric relative humidity, temperature and other atmospheric parameters. If we use U to represent relative humidity, q to represent specific humidity, and T to denote temperature. We can relate the rates of change for T and q to rates of change in relative humidity U at the atmosphere. According to [17], relative humidity at a given temperature is given by the ratio of the actual water vapour pressure e to the saturation vapour e_s at same pressure P and temperature T . It can also be given by the ratio of q to the saturation-specific humidity q_s , the above illustrations can be obtain mathematically as follows

$$U = \frac{e}{e_s} \approx \frac{q}{q_s} \quad (1)$$

The specific humidity q is related to the pressure p and water vapour pressure e by equation (2)

$$q = \varepsilon \frac{e}{p + (1 - \varepsilon)e} \quad (2)$$

$$\text{Mathematically } \frac{e}{p + (1 - \varepsilon)e} < \frac{e}{p},$$

Therefore,

$$q \approx \varepsilon \frac{e}{p} \quad (3)$$

Where $\varepsilon = \frac{R_d}{R_v}$ (≈ 0.622) and, R_d and R_v are the gas constant phases for dry and water vapour. According to $[4] \frac{de_s}{dT} =$

$$\frac{de_s}{R_v T^2} = \frac{1}{R_v} \left[\frac{Le_s}{T^2} \right] = \frac{\varepsilon}{R_d} \left[\frac{Le_s}{T^2} \right] = \varepsilon \frac{Le_s}{R_d T^2} \quad (4)$$

Where e_s is the saturation vapor pressure of water and L_v the latent heat of vaporization. The temperature at which saturation is reached is called the dew point temperature T_d , so at this temperature the actual vapour pressure becomes the saturated value ($e = e_s$). Therefore, equation (4) reduces to

$$\frac{de}{dT_d} = \frac{Le}{R_v R_d^2} \quad (5)$$

Equation 5 shows that T_d and e are humidity parameters that give equivalent information. Integrating equation (4) with respect to T_d and T , and taking the exponent of both side of the equation, we obtain

$$e_s = \exp \left[\frac{L}{R_v} \left(\frac{1}{T_d} - \frac{1}{T} \right) \right] \quad (6)$$

If $T = T_d$, e is the saturation vapour pressure. Equations (1), (3), (4) and (5) form a close system of four variables q , e , U and T_d or q , U , T and T_d etc. Differentiating equation (1) by focusing on the parameters U and assessing its variation with

specific humidity and temperature for an isobaric level ($p = \text{constant}$, that is surface in the atmosphere where the pressure is equal everywhere along that surface), we obtain

$$\frac{dU}{U} = \frac{de}{e} - \frac{de_s}{e_s} = \frac{dq}{q} - \frac{dq_s}{q_s} \quad (7)$$

Differentiating equation (3) using the same approach, we also obtain

$$\frac{dq_s}{q_s} = \frac{de_s}{e_s} - \frac{dp}{p} \quad (8)$$

Since p is a constant, then $dp = 0$, therefore, equation (8) becomes,

$$\frac{dq_s}{q_s} = \frac{de_s}{e_s} \quad (9)$$

Comparing equation (4) and (9), we obtain

$$\frac{de_s}{e_s} = \frac{LdT}{R_v T^2} = \left(\frac{L}{R_v T}\right) \frac{dT}{T} \quad (10)$$

Inserting equation (10) into equation (7), we have

$$\frac{dU}{U} = \frac{dq}{q} - \left(\frac{L}{R_v T}\right) \frac{dT}{T} \quad (11)$$

Equation (11) is the expression relating relative humidity, specific humidity and temperature. The contribution of specific humidity and temperature to relative humidity is in opposite sign. The variation dT may be due to diabatic heating and adiabatic effects [4]. That is, the air cools diabatically through evaporational cooling and warms adiabatically as it sinks to the surface. A parcel of air could be experiencing evaporational cooling at the same time it is sinking and warming adiabatically, the cooling and warming at the same time will try to offset each other. Therefore, with rising adiabatic motion the cooling of the air lowers the value of the saturation water vapour pressure and increases the relative humidity. Again, with sinking the saturation water vapour pressure will increase leading to a decrease in relative humidity. This is because adiabatic process deals with the changing temperature of a parcel of air due to the air rising adiabatically or sinking adiabatically. This shows that U increases, if specific humidity increases and/or temperature decrease [4].

2. Materials and Methods

2.1 Materials

2.1.1 The Study Area

The study areas used in this work are thirty six (36) points station over Nigeria as shown in Figure 1, which is the gridded map of selected stations in Nigeria, while Table 1 shows the coordinates of the selected stations over Nigeria. These stations were selected based on the interval of 1.5° (from one point to the order) of the gridded map to cover Nigeria

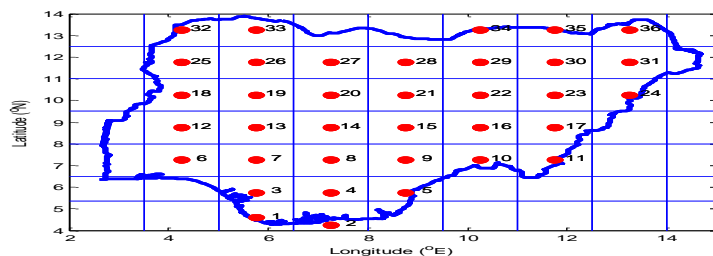


Figure 1: Gridded Map of Nigeria Showing Data Points of the selected stations in Nigeria [18]

2.1.2 Sources of Data

Satellite relative humidity and temperature data used in this study were obtained from web archive of the ERA-INTERIM data. The data which was in NetCDF format were extracted, converted to binary format, sorted and merged to file using MATLAB software program. The data collected were daily data.

2.2 Research Method

2.2.1 Modeling of Neural Network

MATLAB software was used to implement the neural network algorithm for the training in this study. In order to implement this algorithm, the data were normalized by presenting it as input data to the network. Normalization of the data was done using the mapminmax processing function, which is a default for the MATLAB neural network algorithm. A total of 20 neural networks algorithms were used for training. The difference between them is in the number of hidden layer neurons applied (the number of hidden layer neurons were varied from 1 to 20). The architecture used for the training comprises of three main layers; an input layer, a hidden layer and an output layer.

This were 4-20-1, which means 4 neurons in the input layer, 20 neurons in the hidden layer and 1 neuron in the output layer. Prior to training, the entire available data was randomly split into three portions: 70% for the training, 15% for validation and the remaining 15% for testing during the simulation. The performance of the training was tested using root mean square error (RMSE) computed to determine the best network for the study.

Equations (12) - (18), respectively were the mathematical models of the Neural Network architecture use to transfer data from the input layer neurons to the hidden layer neurons and from the hidden layer neurons to the output layer neurons as shown in Figure 2 [18]. The code written for the modeling; that is the training, estimation, correlation, spatial distributions, and extraction of neural network equations can be provided under request. Thus,

$$\sum(I_{wm} * I_m + b_1) = n_1 \tag{12}$$

$$f_1(n_1) = \text{tansig}(n_1) = \frac{e^{n_1} - e^{-n_1}}{e^{n_1} + e^{-n_1}} = H_{vm} \tag{13}$$

The express of Equation (12) is written with MATLAB codes. Hyperbolic tangent sigmoid transfer function (f_1) is applied to Equation (12) to have hidden layer matrix (H_{vm}) (13).

$$\sum(L_{wm} * H_{vm} + b_2) = n_2 \tag{14}$$

The sum of the layer weight matrix multiplying with hidden layer matrix plus the bias vector two (b_2) give Equation (14). Linear function was also applied to Equation (14) to have equation (15). From hidden layer to the output layer we generated the targeted output called the output matrix as expressed in Equation (16) and (17), while combination of Equations (12 – 16) respectively gave straight line Equation (18) (that is, from input matrix to output matrix).

$$f_2(n_2) = \text{purelin}(n_2) = O_m \tag{15}$$

$$f_2(n_2) = \text{purelin}(L_{wm} * H_{vm} + b_2) = O_m \tag{16}$$

$$O_m = L_{wm} * H_{vm} + b_2 \tag{17}$$

$$O_m = L_{wm} * (\text{tansig}(I_{wm} * I_m + b_1)) + B_2 \tag{18}$$

where O_m depicts the output matrix containing the desired outputs. I_m is the input matrix (year, day of the year (DOY), latitude, longitude), I_{wm} depict inputs weight matrix, b_1 is bias vector one, H_{vm} is the hidden variable matrix, L_{wm} is layer weight matrix, b_2 is bias vector two, $\text{tansig}(f_1)$ is hyperbolic tangent sigmoid transfer function used between the input and the hidden layers as activation function, while $\text{purelin}(f_2)$ is the linear transfer function used from hidden layers to the output layer as the activation function. The values of I_{wm} , L_{wm} , b_1 and b_2 of this study are available on request. Figure 3 is the network diagram of the neural network model.

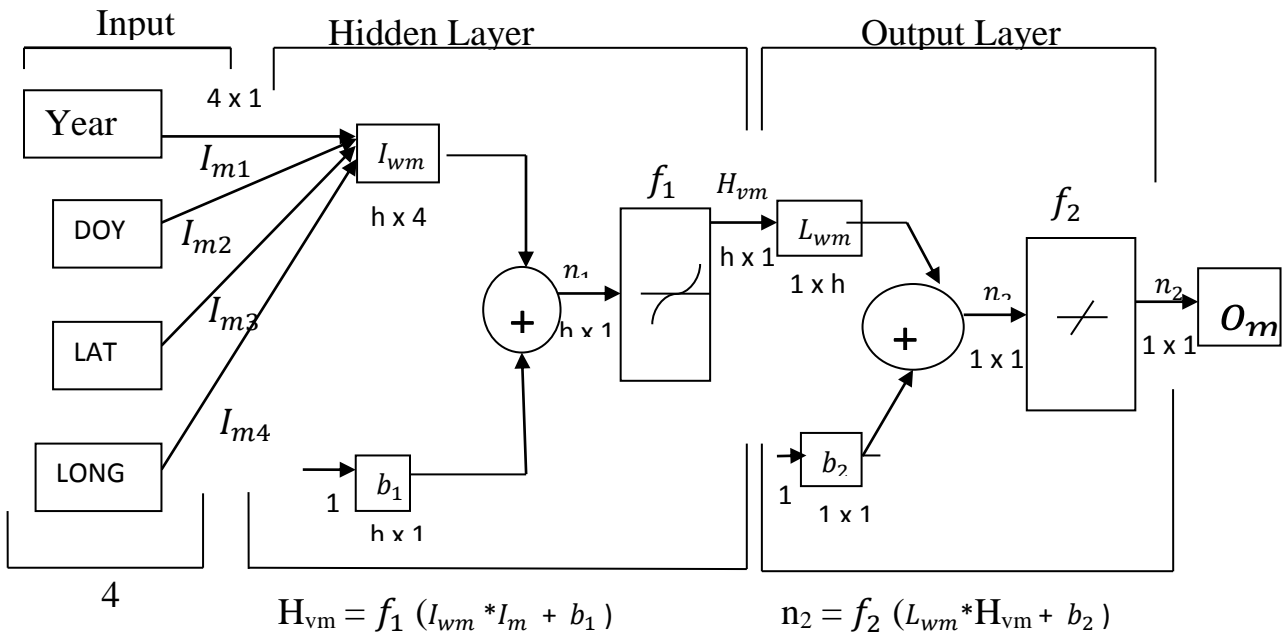


Figure 2: Neural Network Training Structure from Input to Output

The size of I_{wm} is h-by-4 which indicate 4 input layer neurons. The size of L_{wm} is 1-by-h which also indicate one output layer neuron. The sizes of b_1 , n_1 , H_{vm} , b_2 and n_2 are h x 1, h x 1, h x 1, 1 x 1 and 1 x 1 respectively, where h is the number of hidden layer neurons[19].

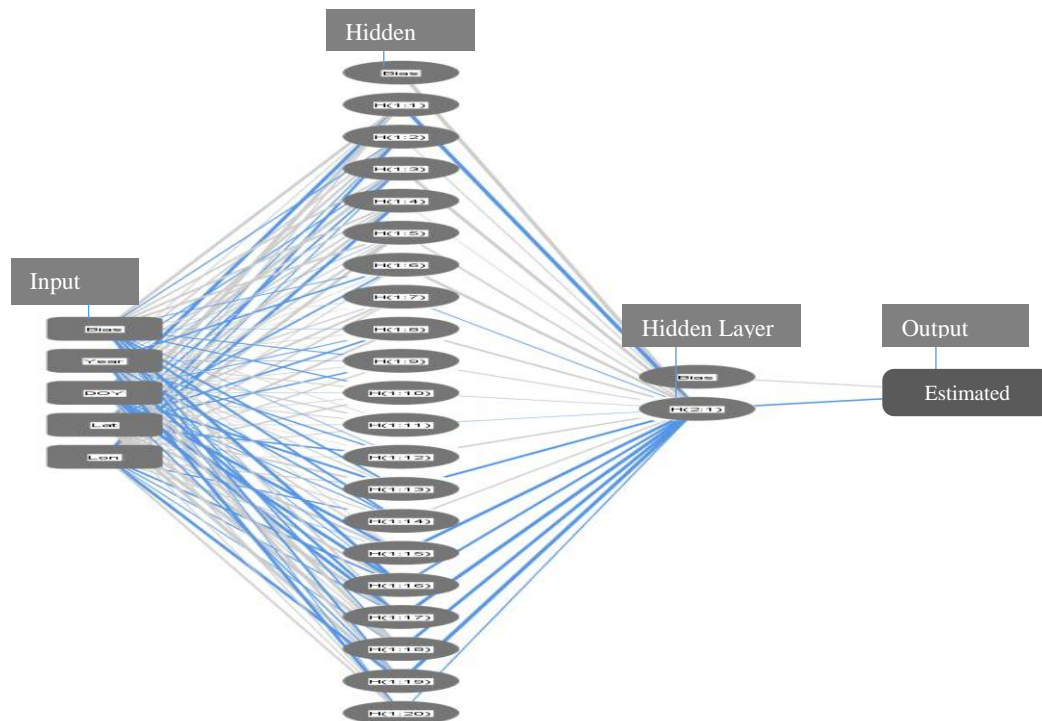


Figure 3: Network Diagram of the Neural Network Model

3.0 Results and Discussion

From Figure 4, the spatial distributions of relative humidity in Nigeria during dry season from 1979 to 2014 showed that a low relative humidity of about 10 – 30 % could be observed in about two-third parts of the country especially in locations around the Central and Northern Nigeria as also revealed by [20]. The high relative humidity of about 35 % and above was obtained in the Southern parts of the country, especially in the Coastal areas. This could be due to high moisture content and low rate of temperature concentration within the Southern region.

For the distribution of temperature in dry season (Figure 5 a – e), it could be observed that for the years under study, the temperature varies from 30 to 40 °C and distributed across the Nigeria. However, the highest temperature concentration of about 34 – 40 °C were obtained dominantly within the Northern part of the country. Comparatively, low temperatures of about 30 – 33 °C are obtained mostly in the South. It is interesting to note that from the Figure, stations with the highest temperature lie along the axes of rivers Niger and Benue. This is because they serve as heat reservoirs during the dry season and hence, the increase in temperature as observed by [19]. In the case of Figure 4, the direction of increase in relative humidity in wet season in Nigeria trends from the South to Northern part of the country. It was observed from the spatial distributions that relative humidity increase significantly across Nigeria in wet season. The increase in the relative humidity in the country in this period could be attributed to the high moisture, heavy rain and low temperature available during the season. Figures 4 and 6 reveal that relative humidity concentrations were higher in the Southern parts of Nigeria compared to the Northern part of Nigeria all through the seasons. This could be attributed to the coastal nature of the region [20, 21]. It is generally observed from Figure 7 (a – e) that in wet season, the temperature ranges between 25 – 45°C, with the ranges of about 35 – 45°C, 32 – 35°C and 25 – 32°C in the Northern, Central and Southern parts of Nigeria, respectively. This is at variance with dry season temperature regimes in those locations. Hence, there is inversion in variations of temperature. The analysis from Figures 4 to 7 revealed that relative humidity is higher in wet seasons compared to dry seasons in Nigeria. It is also higher within the Southern part of Nigeria. The results also shows inversion with the rates of relative humidity and the rates of temperature both in wet and dry seasons, and within the Southern and Northern part of Nigeria.

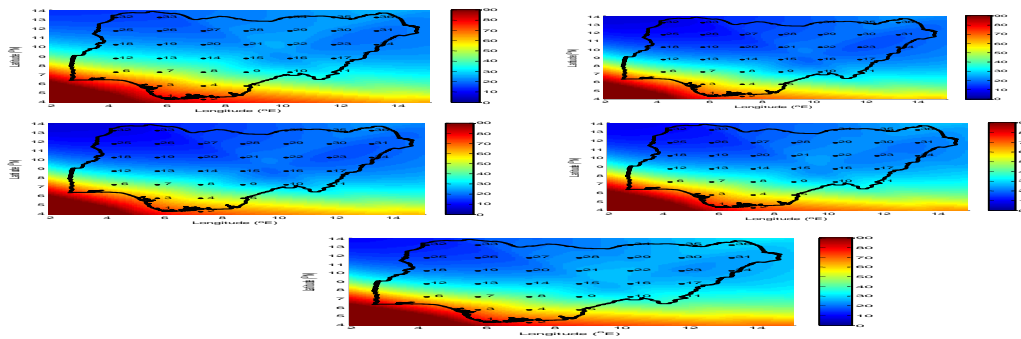


Figure 4: The spatial variations of relative humidity (%) in dry season over Nigeria for the periods: (a) 1979 (b) 1989 (c) 1999 (d) 2009 and (e) 2014.

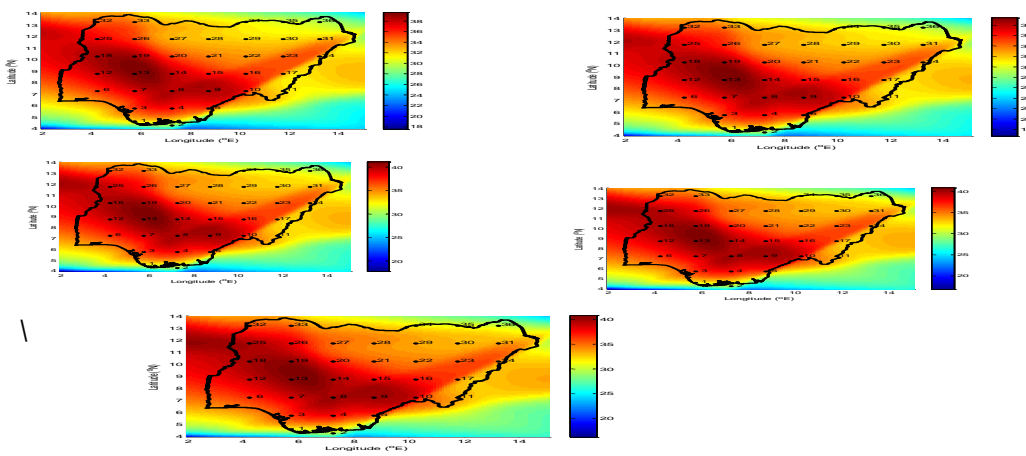


Figure 5: The Spatial Variations in Temperature (°C) in Dry Season over Nigeria for the Periods: (a) 1979 (b) 1989 (c) 1999 (d) 2009 and (e) 2014

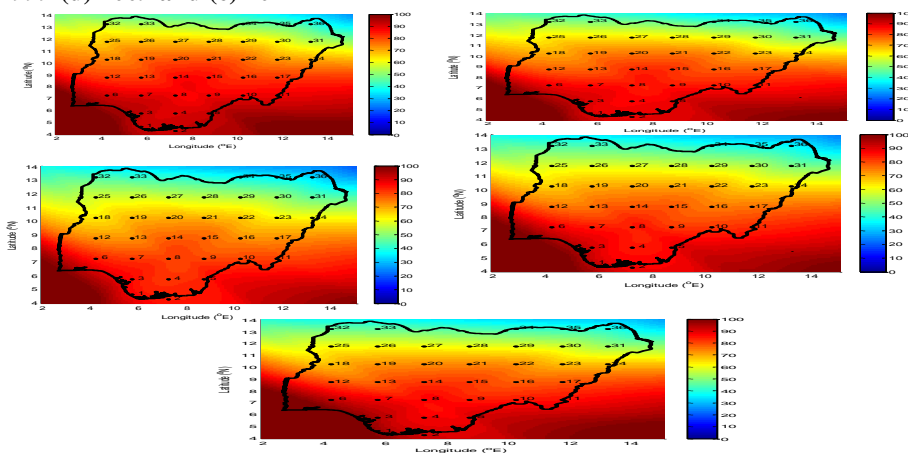


Figure 6: The spatial variations of relative humidity (%) in wet season over Nigeria for the periods: (a) 1979 (b) 1989 (c) 1999 (d) 2009 and (e) 2014

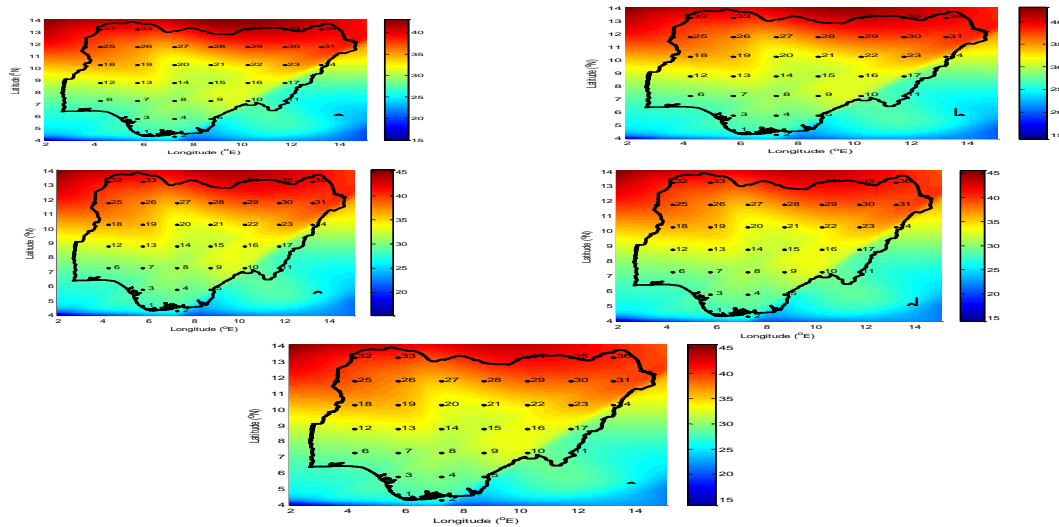


Figure 7: The Spatial Variations in Temperature (°C) in Wet Season over Nigeria for the Periods: (a) 1979 (b) 1989 (c) 1999 (d) 2009 and (e) 2014.

In other to validate the performance of the model used for spatial variations, estimation of the data was carried out in some points from the gridded map. The results were plotted with observed data. Figure 8 gives the trends in the variations of observed and estimated (with the model) values of relative humidity. High relative humidity occurs in the months between April to September and low values occur between October – March as a result of the variations of temperature between wet and dry seasons. The similarities in the signatures of the observed and estimated prove a direct and high correlation between the observed and estimated data. Similarly, the model exhibits good performance in estimating relative humidity since both the estimated and observed have similar signatures.

From Figure 9 (a – f), it could be seen that both estimated and observed temperature data have similar periodic signatures, with peak temperatures occurring in January and October, and least temperature in July. In addition, the similarity in both signatures proves the good performance of the Neural Network model used in estimating the observed data. This confirms high performance of the programmes and models used for the estimation. This is in line with [16] and [22] who stated that impressive performance of the neural networks model supports the application of neural networks in modeling climatic parameters like temperature and relative humidity.

Based on the high performance of the model in the temporal distributions of the parameters, two years ahead of the observed data was predicted. The result in Figures 10, 11, 12 and 13 reveal the 2018 and 2019 temporal distribution of forecast of relative humidity and temperature. The results reveal that the concentrations of both years has similar signature. The distribution shows that the highest concentration relative humidity and lowest concentration of temperature occurs between June-September of both years and locations [23]. This confirmed the result of temporal distributions of observed and estimated relative humidity and temperature. The result shows that neural network has the ability of performing forecast of single and multi-steps ahead of the observed data.

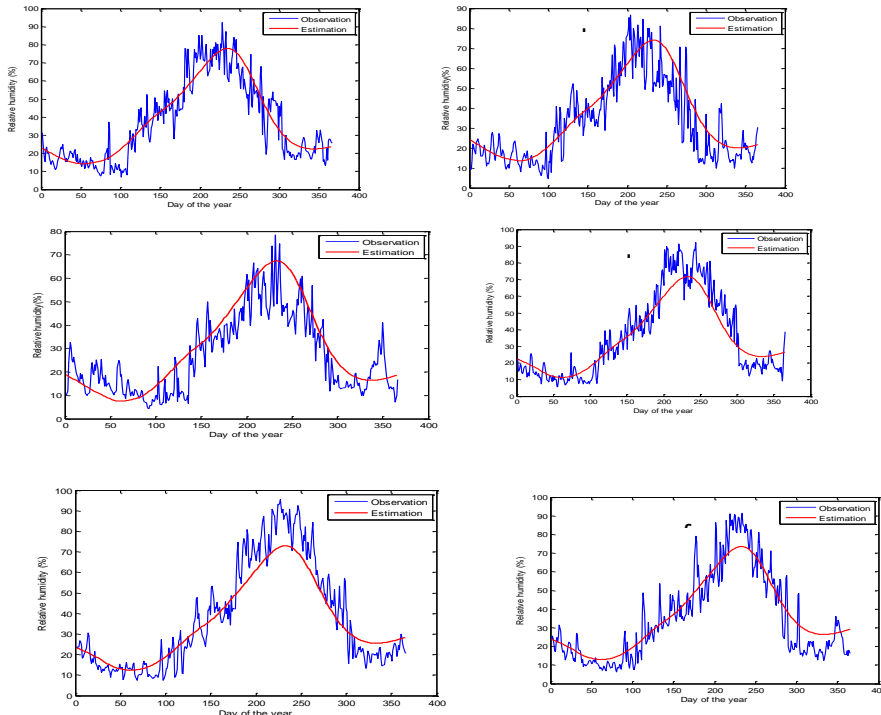


Figure 8: The diurnal variations of observed and estimated relative humidity at (11.75 °N: 11.75 °E) for the periods: (a) 1980 (b) 1990 (c) 2000 (d) 2010 (e) 2012 and (f) 2013.

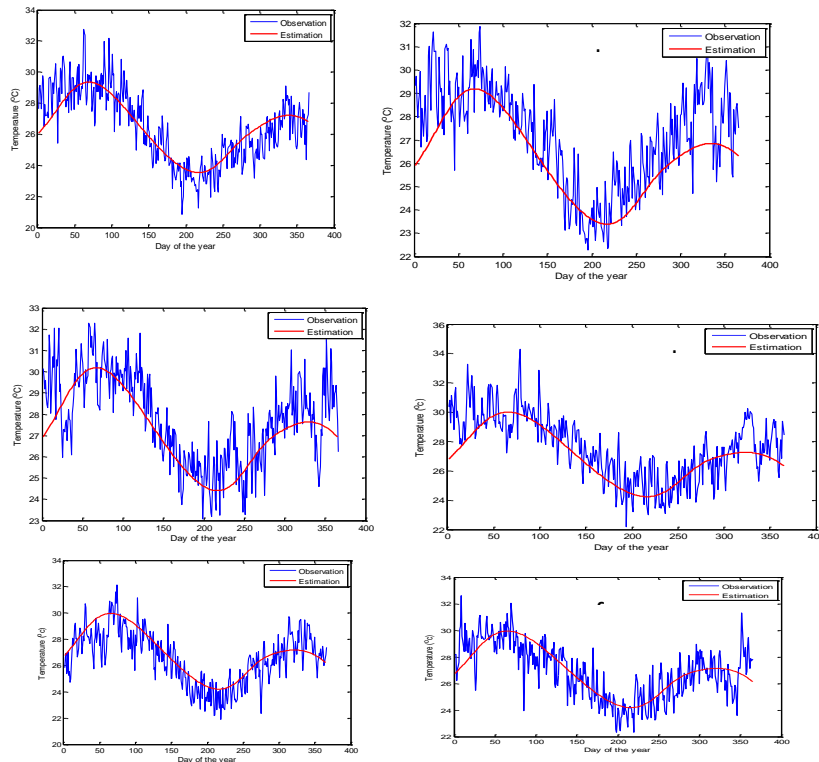


Figure 9: The Diurnal Variations of Observed and Estimated Temperature (10.25 °N: 10.25 °E) for the Periods: (a) 1980 (b) 1990 (c) 2000 (d) 2010 (e) 2012 and (f) 2013

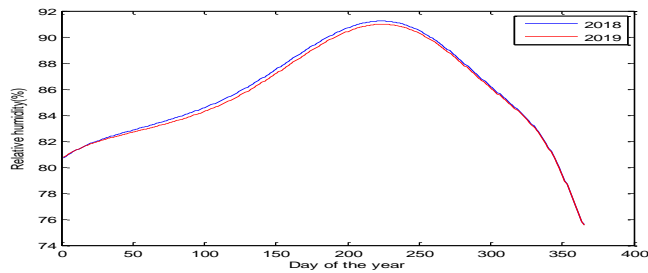


Figure 10: Variation of forecast of 2018 and 2019 at Apoi Creek, Bayelsa State (4.59 °N: 5.84 °E) of relative humidity

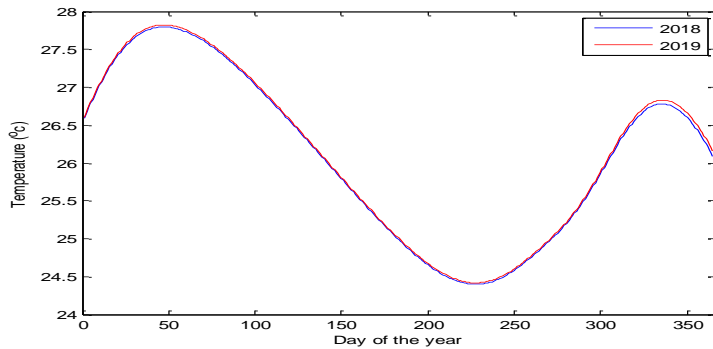


Figure 11: Variations of Forecast of 2018 and 2019 at Apoi Creek, Bayelsa State (4.59 °N: 5.84 °E) for: (G) Methane (H) Carbon (iv) Oxide and (I) Temperature

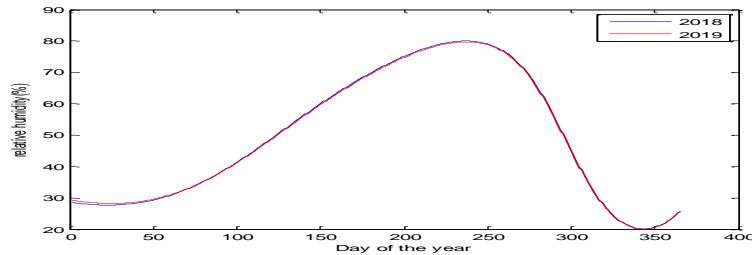


Figure 12: Variation of forecasts of 2018 and 2019 at Danjuma, Taraba State (7.25 °N: 10.25 °E) of relative humidity

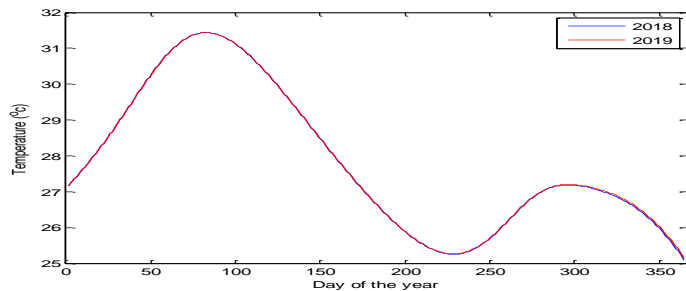


Figure 13: Variations of Forecasts of 2018 and 2019 at Danjuma, Taraba State (7.25 °N: 10.25 °E) For: (G) Methane (H) Carbon (iv) Oxide (I) Temperature

Correlation analysis was carried out in further to evaluate the relationship between temperature and relative humidity. The result showed strong negative relationship between temperature and relative humidity. This implies that temperature is inversely proportional to relative humidity. The correlation coefficient is calculated to be -0.94. This strong negative correlation signifies that as the temperature decreases, the relative humidity increase (and vice versa)

4. Summary and Conclusion

Relative humidity and temperature are among the major atmospheric parameters that influences climate change which result to global warming. Based on this reason, the study in recent time has becomes inevitable. In recent researches, machine learning-based modeling strategies have proven significant attention in tackling the challenges of nonlinear and complex problems of atmospheric modeling. To further the course of research on modeling of atmospheric and climate change in Nigeria, we carried out a study to examine the relationship between relative and temperature on the: spatial distributions of relative humidity and temperature over Nigeria, estimation of the parameters, temporal variations of estimated and observed data at selected point stations of relative humidity and temperature, study the relationship between the parameters and prediction of two years ahead of the parameters of the years under study. Therefore, neural network model were used in this study to affirm the uses of the model in atmospheric analysis, and profiling mathematical model for future study. Overview of the mathematical basis of the general relationship between the relative humidity and temperature were stated in this research. The research study with the titled; “neural network modeling of relative humidity and temperature distributions over Nigeria” gave the following findings.

- (1) The result revealed that temperature and relative humidity in Nigeria are inversely proportional to each other
- (2) Spatio-temporal variations revealed that relative humidity is higher in wet seasons compared to dry seasons in Nigeria
- (3) Relative humidity is higher within the Southern part of Nigeria as a result of coastal nature, moisture content in the atmosphere of the region and low temperature gradient.
- (4) The results shows inversion with the rates of relative humidity and the rates of temperature both in wet and dry seasons, and within the Southern and Northern part of Nigeria.
- (5) The invasion could be because increase in temperature raises saturated vapour pressure, which leads to reduction in the relative humidity
- (6) The variation of temperature may be due to diabatic heating and adiabatic effects in the atmosphere
- (7) The results of the research confirmed high performance of neural network model in studying atmospheric parameters like temperature and relative humidity can be encouraged. It has been therefore recommended for atmospheric research.
- (8) The study concludes that there is a strong negative correlation between the relative humidity and the temperature distributions. The correlation coefficient is calculated to be -0.94.
- (9) This strong negative correlation signifies that as the temperature decreases, the relative humidity increase (and vice versa).

Based on the performance of neural network model in studying Relative Humidity and Temperature Distribution as confirmed by other researchers, neural network model can be used for atmospheric analysis.

DATA AVAILABILITY STATEMENT

Satellite relative humidity and temperature datasets generated and analyzed during the current study are at_web archive of the ERA-INTERIM data

Reference

- [1] Xin L, Wenyong F, Lunche W, Ming L, Rui Y, Shaoqiang W, Lizhe W (2020) Effect of urban expansion on atmospheric humidity in Beijing-Tianjin-Hebei urban agglomeration. *Sci of the Tot Env* 759: 1-2.
- [2] Lawrence MG (2005) The Relationship between Relative Humidity and the Dewpoint Temperature in Moist Air: A Simple Conversion and Applications. *Am Met So* 86 (2): 225-233
- [3] Ibeh GF, Agbo GA, Agbo PE, Ali PA (2012) Application of Neural Network for Global Solar Radiation Forecasting with Temperature. *Adv in Appl Sci Res* 3(1):130-134.

- [4] Heyn I, Quaas J, Salzmann M, Mülmenstädt J (2017) Effects of Diabatic and Adiabatic processes on Relative Humidity in a GCM, and Relationship between Mid-Tropospheric Vertical Wind and Cloud-Forming and Cloud-Dissipating Processes. *Dyn Met and Ocea* 69:1, 1-14. DOI: 0.1080/16000870.2016.1272753
- [5] Kinza Q, Ashfaq A, Muhammad A, Abdul-Sattar N, Moonyong L (2021) Developing Machine Learning Models for Relative Humidity Prediction in Air-Based Energy Systems and Environmental Management Applications. *J of Env Mgt* 292:1-10. DOI: 10.1016/j.jenvman.2021.112736
- [6] Buhari M and Adamu SS (2012) Short-Term Load Forecasting Using Artificial Neural Network. Proceedings of international Multi-Conference of Engineers and Computer Scientists. Vol 1 IMECS Hong Kong 2-14
- [7] Kevin PM (2012) Machine Learning: A Probabilistic Perspective. The MIT Press Cambridge, Massachusetts, London, England. 1-2
- [8] Annina S, Deo MS, Venkatesan S, Ramesh BDR (2015). An overview of Machine Learning and its Applications. *Inter J of Elect Sci and Eng(IJESE)* 1 (1): 22-24.
- [9] Alzubi J, Nayyar A, Kumar A (2018) Machine Learning from Theory to Algorithms: An Overview. *J of Phy: Conf. Series* 1142: 1-15
- [10] Agbulut Ü, Gürel AE, Ergün A, Ceylan I (2020) Performance assessment of a V-trough photovoltaic system and prediction of power output with different machine learning algorithms. *J. Clean. Prod* 268: 1-7. <https://doi.org/10.1016/j.jclepro.2020.122269>.
- [11] Assouline D, Mohajeri N, Scartezzini J (2018) Large-scale rooftop solar photovoltaic technical potential estimation using Random Forests. *Appl. Energy* 217: 189–211. <https://doi.org/10.1016/J.APENERGY.2018.02.118>.
- [12] Li Y, Zou C, Berecibar M, Nanini-Maury E, Chan JCW, Van DBP, Mierlo J, Omar N (2018) Random forest regression for online capacity estimation of lithium-ion batteries. *Appl. Energy* 232: 197–210. <https://doi.org/10.1016/j.apenergy.2018.09.182>.
- [13] Yang Q, Yuan Q, Li T, Yue L (2020) Mapping PM_{2.5} concentration at high resolution using a cascade random forest based downscaling model: evaluation and application. *J. Clean. Prod* 277: 1-7. <https://doi.org/10.1016/j.jclepro.2020.123887>
- [14] Beale MH, Haagan MT, Demuth BH (2014) Neural Network Toolbox™. User's Guide (R2014b) USA, The Math Works, Incorporation Pp 10-40
- [15] Sheela KG, Deepa SN (2013) A new algorithm to find number of hidden neurons in Radial Basis Function Networks for wind speed prediction in renewable energy systems. *Con Eng Appl Inf* 15(3): 30-37.
- [16] Daniel O, Najib Y, Oluwaseye A, Ibrahim M, Bababtunde R (2015) Preliminary results of temperature modeling in Nigeria using neural networks. *Roy Met Soci* (70): 336-342.
- [17] Maitha HSA, Ali HA, Hassan ANH (2011) Using MATLAB to Artificial Neural Network Models for Predicting Global Solar Radiation in Al Ain City–UAE Using MATLAB code. *Engineering Education and Research Using MATLAB* 9: 220-238
- [18] Ibeh G. F, Udochukwu B. C, Ibeh L. M and Okoh D (2020). Evaluation of methane emission distributions in Nigeria using neural network model. **Climate Change - Disc Scie Soc, 6 (21).**
- [19] Ibeh GF, Udochukwu BC, Igbawua T, Tyovenda A, Ofoma JN (2019) Assessment of Global Solar Radiation at Selected Points in Nigeria Using Artificial Neural Network Model (ANNM). *Inter J of Env and Clim Ch* 9(7): 376-390
- [20] Eludoyin OM (2011) Air Temperature and Relative Humidity Areal Distribution over Nigeria. *IFE Res Pub in Geo* 10(1): 134 – 145
- [21] Ajadi DA, Sanusi YK (2013) Effect of Relative Humidity on Oven Temperature of Locally Design Solar Cabinet Dryer. *Glob J of Sci Front Res Phy and Spa Sci* 13 (1): 13-17

- [22] Mawonike R, Mandonga G (2017). The Effect of Temperature and Relative Humidity on Rainfall in Gokwe Region, Zimbabwe: A Factorial Design Perspective. *Inter J of Mult Aca Res* 5 (2): 2309-3218
- [23] Jirasuwankul N (2018) Visualization and Estimation of Temperature from Glowing Hot Object by Artificial Neural Network and Image Analysis Technique. The 8th International Conference on Sustainable Energy Information Technology (SEIT 2018), *Sci Dir Procedia Comp Sci* 130: 712–719

